The Plant Cell, Vol. 17, 2157–2171, August 2005, www.plantcell.org © 2005 American Society of Plant Biologists

RESEARCH ARTICLES

The Putative RNA-Dependent RNA Polymerase *RDR6* Acts Synergistically with *ASYMMETRIC LEAVES1* and *2* to Repress *BREVIPEDICELLUS* and MicroRNA165/166 in Arabidopsis Leaf Development [W]

Hong Li,[a,1] Lin Xu,[a,b,1] Hua Wang,[a] Zheng Yuan,[a] Xiaofeng Cao,[c] Zhongnan Yang,[d] Dabing Zhang,[b] Yuquan Xu,[b] and Hai Huang[a,2]

[a] National Laboratory of Plant Molecular Genetics, Shanghai Institute of Plant Physiology and Ecology, Shanghai Institute for Biological Sciences, Graduate School of Chinese Academy of Sciences, Shanghai 200032, China
[b] College of Life Science and Biotechnology, Shanghai Jiao Tong University, Shanghai 200030, China
[c] Institute of Genetics and Developmental Biology, Chinese Academy of Sciences, Beijing 100101, China
[d] College of Life and Environment Sciences, Shanghai Normal University, Shanghai 200234, China

The *Arabidopsis thaliana ASYMMETRIC LEAVES1* (*AS1*) and *AS2* genes are important for repressing class I *KNOTTED1*-like homeobox (*KNOX*) genes and specifying leaf adaxial identity in leaf development. RNA-dependent RNA polymerases (RdRPs) are critical for posttranscriptional and transcriptional gene silencing in eukaryotes; however, very little is known about their functions in plant development. Here, we show that the Arabidopsis *RDR6* gene (also called *SDE1* and *SGS2*) that encodes a putative RdRP, together with *AS1* and *AS2*, regulates leaf development. *rdr6* single mutant plants displayed only minor phenotypes, whereas *rdr6 as1* and *rdr6 as2* double mutants showed dramatically enhanced *as1* and *as2* phenotypes, with severe defects in the leaf adaxial-abaxial polarity and vascular development. In addition, the double mutant plants produced more lobed leaves than the *as1* and *as2* single mutants and showed leaf-like structures associated on a proportion of leaf blades. The abnormal leaf morphology of the double mutants was accompanied by an extended ectopic expression of a class I *KNOX* gene *BREVIPEDICELLUS* (*BP*) and high levels of microRNA165/166 that may lead to mRNA degradation of genes in the class III HD-ZIP family. Taken together, our data suggest that the Arabidopsis *RDR6*-associated epigenetic pathway and the *AS1-AS2* pathway synergistically repress *BP* and *MIR165/166* for proper plant development.

INTRODUCTION

In higher plants, leaf primordia initiate from flanks of the shoot apical meristem (SAM) (Bowman et al., 2002). The initiation of leaf primordia coincides with the downregulation of the expression of several class I *KNOTTED1*-like homeobox (*KNOX*) genes (Byrne et al., 2000; Ori et al., 2000; Semiarti et al., 2001), which are required for the maintenance and growth of the SAM (Long et al., 1996; Bowman and Eshed, 2000; Volbrecht et al., 2000). Leaf development also requires the establishment of proximodistal, mediolateral, and adaxial-abaxial polarities (Hudson, 2000). The adaxial-abaxial polarity refers to the two opposing faces of a leaf blade, which have distinct cell types that have different biological functions (McConnell et al., 2001). It was reported that leaf primordia isolated from the SAM at the anlage stage could only form a small radial leaf without adaxial differentiation (Sussex, 1954, 1955). This result indicates that the establishment of the adaxial-abaxial axis is critical for subsequent asymmetric leaf development (Bowman et al., 2002).

In *Arabidopsis thaliana*, several genes have been identified for the formation of the adaxial-abaxial polarity, including class III HD-ZIP genes for promoting adaxial fate (McConnell and Barton, 1998; McConnell et al., 2001; Emery et al., 2003) and members of the *YABBY* and *KANADI* families for specifying leaf abaxial identity (Chen et al., 1999; Sawa et al., 1999; Siegfried et al., 1999; Eshed et al., 2001; Kerstetter et al., 2001). In addition, the *ASYMMETRIC LEAVES1* (*AS1*) and *AS2* genes are also responsible for establishing leaf polarity by specifying leaf adaxial identity (Xu et al., 2002, 2003). *AS1* encodes a protein that contains an R2-R3 MYB domain (Byrne et al., 2000; Sun et al., 2002), suggesting that it may bind to DNA. *AS2* encodes a plant-specific protein that can associate with AS1 (Iwakawa et al., 2002; Xu et al., 2002, 2003). These two genes have demonstrated roles in repressing class I *KNOX* genes (Byrne et al., 2000; Ori et al., 2000; Semiarti et al., 2001) and promoting leaf vein development (Semiarti et al., 2001; Sun et al., 2002). Recent

[1] These authors contributed equally to this work.
[2] To whom correspondence should be addressed. E-mail hhuang@sippe.ac.cn; fax 86-21-54924015.
The author responsible for distribution of materials integral to the findings presented in this article in accordance with the policy described in the Instructions for Authors (www.plantcell.org) is: Hai Huang (hhuang@sippe.ac.cn).
[W] Online version contains Web-only data.
Article, publication date, and citation information can be found at www.plantcell.org/cgi/doi/10.1105/tpc.105.033449.

studies have also revealed that in early leaf development, *AS1* and *AS2* are required for a proper auxin distribution and response (Zgurski et al., 2005). Additionally, *AS1* and *AS2* positively regulate the *PHABULOSA* (*PHB*) gene, a class III HD-ZIP family member (Lin et al., 2003; Xu et al., 2003). Although *AS1* and *AS2* functions have been studied extensively, it is unclear whether other genes function together with *AS1* and *AS2* for leaf patterning. If these genes exist, it would therefore be important to determine what roles they play in leaf development.

In both plants and animals, double-stranded RNA (dsRNA) that is processed to short RNAs (~21 to 24 nucleotides) can trigger two coupled types of RNA-mediated gene silencing events: posttranscriptional gene silencing (PTGS) and transcriptional gene silencing (TGS) (Cogoni and Macino, 1999; Lipardi et al., 2001; Matzke et al., 2001; Nishikura, 2001; Sijen et al., 2001; Ahlquist, 2002; Aufsatz et al., 2002). Members of the RNA-dependent RNA polymerase (RdRP) family use small RNA molecules to prime dsRNA synthesis (Lipardi et al., 2001; Sijen et al., 2001) and have been defined as one of the important factors in PTGS and TGS. In recent years, genes encoding putative RdRPs have been isolated and characterized from several species, including tomato (*Lycopersicon esculentum*), *Neurospora crassa*, *Caenorhabditis elegans*, and Arabidopsis (Schiebel et al., 1993, 1998; Cogoni and Macino, 1999; Dalmay et al., 2000; Mourrain et al., 2000; Smardon et al., 2000). In Arabidopsis, mutations in the *RDR6* gene, which encodes a putative RdRP protein, causes defects in PTGS (Dalmay et al., 2000; Mourrain et al., 2000). In addition, a more recent study revealed that the *RDR6* gene is required for vegetative phase change (Peragine et al., 2004). However, because *rdr6* mutant plants do not show severe morphology defects, the role of RdRPs in leaf pattern specification is largely unknown.

MicroRNAs (miRNAs) are endogenous ~20- to 22-nucleotide RNAs that contribute important functions in animal and plant development by causing mRNA cleavage or protein translational repression (Bartel, 2004). The Arabidopsis miRNAs miR165 and miR166 differ by only one nucleotide and were found to share perfect complementarity with the regions of class III HD-ZIP genes encoding the START domain (Rhoades et al., 2002). A single nucleotide change within the START-encoding regions of some of these genes resulted in dominant mutations that caused aberrant adaxial-abaxial polarity and abnormal venation in leaves (McConnell et al., 2001; Emery et al., 2003; Zhong and Ye, 2004). Recent in vitro and in vivo experiments have shown that miR165/166 can indeed cause degradation of mRNAs of several HD-ZIP genes (Emery et al., 2003; Tang et al., 2003; Mallory et al., 2004; Zhong and Ye, 2004). Studies investigating the mechanisms of miRNA actions raise an important question: what gene(s) or pathway(s) regulates the level of miRNA gene expression in developmental processes? It was reported that the Arabidopsis gene *ARGONAUTE1* (*AGO1*) both acts in and is regulated by the miRNA pathway (Kidner and Martienssen, 2004; Vaucheret et al., 2004). However, it is not clear whether other factors are also involved in the regulation of miRNA expression.

In this study, we describe the characterization of *rdr6* single mutants and *rdr6 as2* double mutants, which suggest a novel function of the previously reported *RDR6* gene in leaf development. We report that the ectopic expression of a class I *KNOX* gene *BREVIPEDICELLUS* (*BP*) was extended and that miR165/166 levels were dramatically increased in the *rdr6 as2* mutant leaves. We propose that the *AS1-AS2* pathway and the *RDR6*-associated epigenetic pathway are both required for repression of *BP* and *MIR165/166* in normal leaf development.

RESULTS

RDR6 Is Involved in Leaf Development

To identify additional genes functioning in the *AS1-AS2* regulatory network, we conducted a genetic screen for enhancers and suppressors of the *as2-101* mutant and identified two mutants showing similar enhanced *as2* phenotypes. Genetic experiments revealed that these two mutants were allelic, and the single *as2* enhancer mutant had nearly normal phenotypes (see Methods). We mapped this enhancer mutation to a 21-kb region on chromosome 3 (BAC T9C5), which contains seven predicted genes (Figure 1A). Sequencing of these candidate genes revealed that both of the *as2* enhancer alleles carried mutations that introduce stop codons into the coding sequence of the *RDR6*, *SDE1*, or *SGS2* genes (in this study, we refer to this gene as *RDR6* for convenience), which encodes a previously reported RdRP protein (Figure 1B). Complementary experiments confirmed that mutations in the *RDR6* gene caused an enhancement of *as2* phenotypes (see Methods); we therefore renamed the *as2* enhancer alleles as *rdr6-3 as2-101* and *rdr6-4 as2-101*, respectively.

RDR6 expression was found in all plant tissues examined (Figure 1C). The molecular genetics relationship between *RDR6* and *AS1*/*AS2* suggests that these genes may influence each other's expression. Therefore, we analyzed *RDR6* expression in the *as1-101* and *as2-101* backgrounds and *AS1* and *AS2* expression in the *rdr6-3* background (Figure 1D). The RT-PCR data revealed no obvious changes between the wild type and mutants, suggesting that direct transcriptional regulations do not occur between the *RDR6* and *AS1* and *AS2* genes. These results indicate that the *RDR6* gene may act separately from the *AS1*/*AS2* pathway in the regulation of plant development.

Phenotypes of *rdr6* Single Mutants and *rdr6 as2* Double Mutants

To further understand the role of *RDR6* in leaf development, we analyzed leaf phenotypes of *rdr6-3 as2-101* plants. Compared with wild-type (Figure 2A) and *as2-101* (Figure 2B) plants, *rdr6-3 as2-101* (Figure 2C) and *rdr6-4 as2-101* (Figure 2D) displayed severe phenotypes, with anthocyanin in some early-appearing rosette leaves. In addition, *rdr6-3 as1-101* and *rdr6-3 as2-101* double mutants showed similar phenotypes (Figure 2E). Because AS1 and AS2 can form protein complexes and may regulate the same downstream targets, the similar phenotypes in *rdr6-3 as1-101* and *rdr6-3 as2-101* suggest that the *RDR6* gene or its product interacts with the *AS1-AS2* pathway in leaf development. Because *rdr6-3 as2-101* and *rdr6-4 as2-101* exhibited similar overall phenotypes, we focused our additional phenotypic

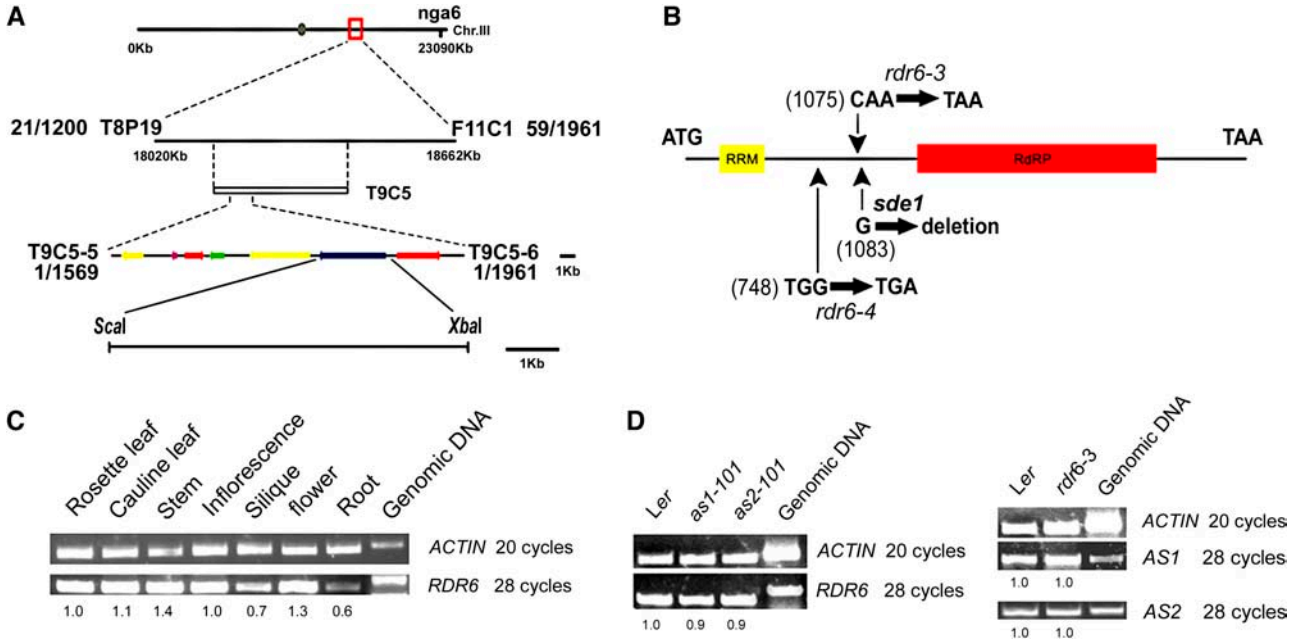

Figure 1. Molecular Identification of the *AS2 ENHANCER1* Gene.

(A) Fine-structure mapping. Seven putative genes (denoted by arrows) were identified between markers T9C5-5 and T9C5-6. The *Sca*I-*Xba*I genomic fragment containing the *RDR6* gene was used in the complementation experiment.

(B) The *RDR6* gene structure and positions of the nucleotide changes in *rdr6-3*, *rdr6-4*, and *sde1-1* mutants. The yellow box indicates a region encoding the RNA recognition motif, and the red box represents a region encoding the RdRP domain (http://www.ncbi.nlm.nih.gov/BLAST).

(C) RT-PCR shows that *RDR6* was expressed in all plant tissues examined.

(D) *RDR6* expression was not affected by *as1* and *as2* mutations, and *rdr6* mutation did not alter expression of the *AS1* or *AS2* genes. The numbers in **(C)** and **(D)** indicate the relative abundance of gene transcripts, which were calculated using the band intensity of the first lane as 1.0. *as1-101*, *as2-101*, and *rdr6-3* are in the L*er* genetic background.

characterizations mainly on the *rdr6-3* and *rdr6-3 as2-101* mutants.

The *rdr6-3* plants displayed only minor phenotypes, including a slightly reduced plant stature with slightly distorted young rosette leaves (Figure 2F) and an increased number of secondary inflorescences (8.9 ± 1.0 in the *rdr6-3* mutant versus 5.9 ± 1.0 in the wild type, $n = 20$, $P < 0.01$). In addition, some *rdr6-3* plants produced an extra small inflorescence at the base of some secondary inflorescences (Figure 2G; 34 small inflorescences/120 *rdr6-3* plants; none were found in 100 wild-type plants). Furthermore, many *rdr6-3* plants produced secondary inflorescences without a cauline leaf or with a variously sized filamentous structure at their proximal ends (Figure 2H; 118/242 *rdr6-3* plants; 3/100 wild-type plants).

Analysis of the previously isolated *sde1-1* single mutant (allelic to *rdr6*) revealed that although *sde1-1* and *rdr6-3* are from different ecotypes, they produce similar morphological abnormalities (Figures 2I and 2J; for comparison, see Figures 2G and 2H). In addition, plants with phenotypes similar to those of *rdr6-3 as2-101* and *rdr6-4 as2-101* mutant plants (Figures 2C and 2D) were observed in the F2 progeny of a cross between *sde1-1* and *as2-101* mutants (data not shown). Phenotypic analyses of the *rdr6* mutant plants indicate that although *rdr6* mutant phenotypes were relatively mild, the *RDR6* gene has multiple functions in development (Figure 2K).

rdr6 as2 Exhibits Extended Ectopic Expression of *BP*

AS1 and *AS2* repress the *KNOX* genes during leaf development, and leaves of some *as1* and *as2* alleles are serrated or even lobed because of the ectopic expressions of *KNOX* genes (Ori et al., 2000; Semiarti et al., 2001). Because the *rdr6-3 as2-101* plants showed more lobed leaves (0 in 44 *as2-101* plants and 32 in 44 *rdr6-3 as2-101* plants), we examined by analyzing leaf morphology and expression of a class I *KNOX* gene *BP* in *as2* and *rdr6 as2* leaves whether *RDR6* is also involved in repressing *KNOX* genes. We found that ectopic leaf primordia appeared frequently on the adaxial side of *rdr6-3 as2-101* leaves (Figure 3A), and some of the ectopic leaf primordia eventually formed leaf-like structures (Figure 3B; 4 in 44 *rdr6-3 as2-101* plants). To examine whether the expression of *BP* was altered in the *rdr6-3 as2-101* leaves, we introduced a *BP*:β-glucuronidase (*GUS*) fusion into *rdr6-3*, *as2-101*, or *rdr6-3 as2-101* plants by crosses and examined GUS staining in these mutant plants. *BP* was repressed in wild-type (Figure 3C) and *rdr6-3* leaves (data not shown), whereas it was expressed in both *as2-101* (Figure 3D) and *rdr6-3 as2-101* leaves (Figure 3E), especially in sinuses of leaf lobes and leaf veins (Figures 3D, 3E, 3G, and 3H). In *rdr6-3 as2-101* leaves, GUS staining was also observed in the ectopic leaf primordium (Figure 3F). Interestingly, *BP* was expressed strongly at the distal ends of each major leaf vein (Figures 3E and

3H) of the double mutants, but this pattern was not observed in the *as2-101* single mutant (see Supplemental Figure 1 online). These *BP* expression observations suggest that *RDR6* may negatively regulate *BP* in *as2-101* mutant leaf blades.

rdr6 as2 Has Severe Defects in Leaf Vein Formation and Adaxial-Abaxial Polarity

Leaf vein development is severely affected in the *as1* and *as2* mutants (Semiarti et al., 2001; Sun et al., 2002). To determine whether *RDR6* is involved in regulating vein formation, we examined the leaves, sepals, and petals of the *as2-101* and *rdr6-3 as2-101* plants. Venations in all *rdr6-3* leaves, sepals, and petals were similar to those in wild-type plants but showed a simple pattern in the *as2-101* mutant (Figures 4A to 4D). The venation pattern in the *rdr6-3 as2-101* mutant was even simpler than that of the *as2-101* single mutant (Figures 4A to 4D). To gain more detailed information of leaf vein development, we analyzed the secondary and tertiary veins by scoring the number of branching points (NBPs) (Hamada et al., 2000). NBPs were found to be dramatically reduced in *rdr6-3 as2-101* leaves, especially in the fine veins (Figures 4E and 4F). These results indicate that *RDR6* is also involved in the vascular development of lateral organs.

We reported previously that the *as2-101* mutant is defective in leaf adaxial-abaxial polarity, showing abaxialized lotus- and needle-like leaves (Xu et al., 2002, 2003). To determine whether *RDR6* plays a role in the adaxial-abaxial polarity formation of lateral organs, we analyzed leaf phenotypes of *rdr6-3 as2-101* by scanning electron microscopy. Similar to the *as2-101* mutant,

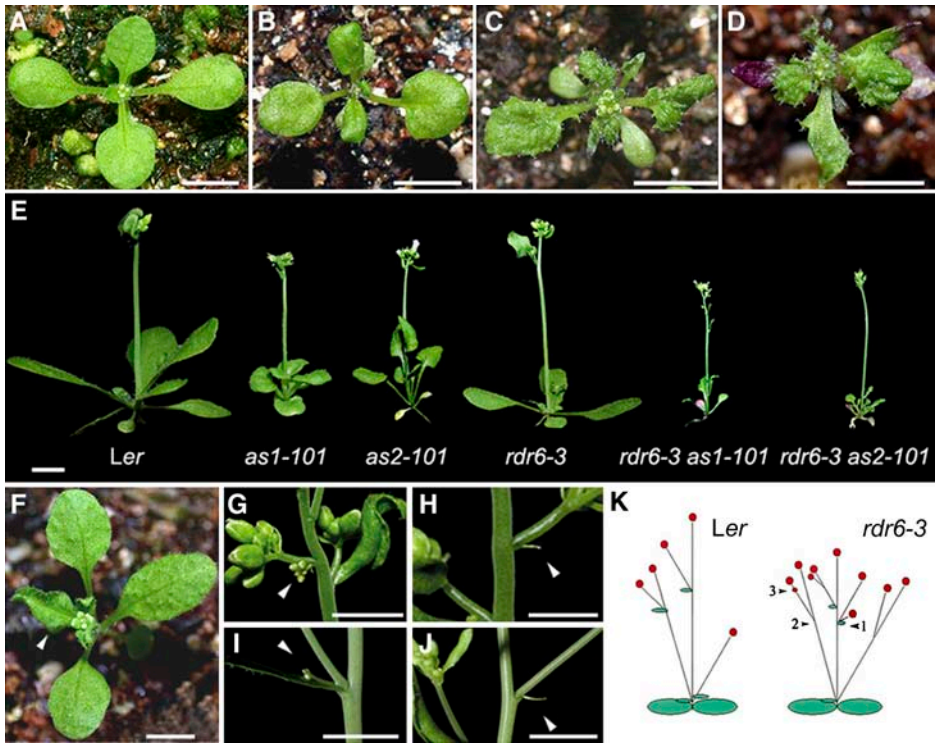

Figure 2. Phenotypes of Single and Double Mutants.

(A) to **(D)** Morphological observations of wild-type and mutant seedlings. Wild-type L*er* **(A)**, *as2-101* **(B)**, *rdr6-3 as2-101* **(C)**, and *rdr6-4 as2-101* **(D)**.
(E) Statures of wild-type, *as1-101*, *as2-101*, *rdr6-3*, *rdr6-3 as1-101*, and *rdr6-3 as2-101* plants at the early flowering stage. Note that *rdr6-3 as1-101* and *rdr6-3 as2-101* plants display similar phenotypes.
(F) *rdr6-3* plants display distorted young rosette leaves (arrowhead).
(G) and **(H)** *rdr6-3* (L*er* ecotype) plants show some minor phenotypic changes.
(G) An additional inflorescence appears at the proximal end of some secondary inflorescences (arrowhead).
(H) Some cauline leaves are replaced by a filamentous structure (arrowhead).
(I) and **(J)** Phenotypic alterations of the previously reported *sde1-1* mutant (Columbia-24 [Col-24] ecotype).
(I) An additional small inflorescence (arrowhead) that is similar to that of *rdr6-3* in **(G)**.
(J) A filamentous structure (arrowhead) appeared at the position where a cauline leaf should grow in the wild-type plants.
(K) A diagram summarizing the phenotypic changes observed in the *rdr6-3* mutant. The *rdr6-3* mutant shows a slightly reduced plant stature. Arrowheads indicate the following abnormalities: (1) additional inflorescence, (2) without cauline leaves or with a small filamentous structure, and (3) with some class IV inflorescences that were not seen in wild-type plants. Red circles indicate inflorescences.
All mutant plants except *sde1* (Dalmay et al., 2000) in **(I)** and **(J)** are in the L*er* genetic background. Bars = 5 mm in **(A)** to **(J)**.

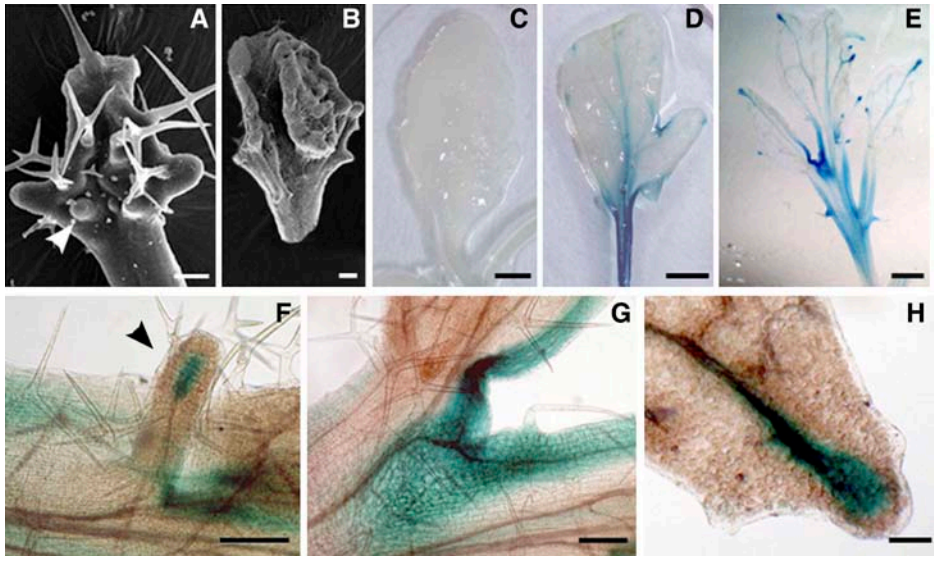

Figure 3. Phenotypes of Early Leaves and *BP* Expression in *rdr6-3 as2-101* Mutant Plants.

(A) A young *rdr6-3 as2-101* leaf showing primordium-like structures on the adaxial side (arrowhead).
(B) Some of the ectopic primordia on the leaf blade can eventually form a leaflet structure.
(C) Wild-type leaves carrying *BP*:*GUS* did not show any GUS activity.
(D) and **(E)** GUS staining was visible in sinuses of leaf lobes and major leaf veins in *as2-101* **(D)** and *rdr6-3 as2-101* mutants **(E)**. Note that some rosette leaves of *as2-101* in a mixed Col-L*er* background contained lobes.
(F) to **(H)** Close-ups of GUS staining in *rdr6-3 as2-101* mutant leaves.
(F) GUS activity was shown at the tip of a major vein (arrowhead) in an ectopic leaf primordium.
(G) GUS staining in sinuses of leaf lobes.
(H) GUS staining at the tip of a major leaf vein.
Leaves in **(A)** and **(B)** were from mutant plants in the L*er* background, and leaves or leaf tissue in all other images were from the F2 plants of a cross between *as2-101 rdr6-3* (L*er*) and a transgenic line carrying the *BP*:*GUS* fusion (Col). Bars = 80 μm in **(B)**, 100 μm in **(F)** and **(H)**, 200 μm in **(A)** and **(G)**, 2 mm in **(C)** and **(D)**, and 1 mm in **(E)**.

we observed lotus-like (Figure 5A) and needle-like (Figure 5B) structures among *rdr6-3 as2-101* rosette leaves but with a much higher frequency in *rdr6-3 as2-101* than in *as2-101* (90% versus 15% of the first-pair rosette leaves). The needle-like leaves in *rdr6-3 as2-101* showed long and narrow epidermal cells (Figure 5B) similar to those of *as2* (Xu et al., 2003) and *phantastica* (*phan*) (Waites and Hudson, 1995) but different from those of *phb-1d* (McConnell and Barton, 1998) and *35S*:*AS2* transgenic plants (Xu et al., 2003), suggesting that these leaves are abaxialized. In the *as2-101* single mutants, lotus- and needle-like leaves only appeared in the first pair of rosette leaves. Strikingly, the *rdr6-3 as2-101* plants showed lotus- and needle-like structures at all positions of rosette leaves, and even some cauline leaves were needle like (data not shown).

The vascular patterns in a series of sections of petioles at the position close to the blade were examined (Figure 5A, white line). In wild-type petioles, xylem develops on the adaxial pole of the vascular bundle, whereas phloem develops on the abaxial bundle pole (Figure 5C). By contrast, *rdr6-3 as2-101* showed ectopic development of abaxial phloem tissue surrounding the xylem in petiole (Figure 5D), which is consistent with the view that *rdr6-3 as2-101* leaves are abaxialized.

To further test the hypothesis that *RDR6* function is required for adaxial-abaxial polarity formation of lateral organs, we analyzed leaf epidermal cells from the *rdr6-3 as2-101* mutant. The adaxial epidermis of wild-type Landsberg *erecta* (L*er*) leaves was characterized by an undulating surface composed of uniformly sized cells (Figure 5E), and the abaxial epidermis was characterized by smaller and less uniformly sized cells (Figure 5F; McConnell and Barton, 1998; Xu et al., 2003). The expanded leaves of *as1* and *as2* and all *rdr6-3* leaves showed a similar epidermal pattern to that of wild-type plants (data not shown). By contrast, the adaxial side of *rdr6-3 as2-101* mutant leaves contained both adaxial epidermal cells (Figure 5G) and patches of abaxialized cells (Figures 5I and 5J). Cells in these patches were similar to those on the abaxial side of both the wild-type (Figure 5F) and *rdr6-3 as2-101* leaves (Figure 5H). The mosaic adaxial-abaxial cells on the adaxial side of a lamina were also observed in the *phan* mutant leaves in *Antirrhinum majus* (Waites and Hudson, 1995) but not seen in *as1* or *as2* alleles. Interestingly, petals of *rdr6-3 as2-101* also demonstrated a severe defect of adaxial-abaxial polarity, which was not observed in the *as2-101* and *rdr6-3* single mutants (data not shown). Wild-type adaxial petal epidermis shows cone-shaped cells with straight lines (Figure 5K), whereas the abaxial petal epidermis shows cobblestone-shaped cells with wavy lines (Figure 5M). Adaxial epidermal cells in the *rdr6-3 as2-101* petals (Figure 5L) were different from those in the wild type (Figure 5K) but rather similar

to the abaxial epidermal cells of petals in both wild-type (Figure 5M) and *rdr6-3 as2-101* double mutant plants (Figure 5N). Phenotypes of leaves and petals in the *rdr6-3 as2-101* mutant plants further support the hypothesis that *RDR6* function is required, along with the *AS1-AS2* pathway, for adaxial-abaxial polarity formation.

In addition to the enhancement of *as2* abnormalities observed in leaves and petals, the *rdr6-3 as2-101* mutant also showed other abnormal phenotypes. These included a markedly slowed growth of leaf primordia (Figures 6A to 6D) and defective floral organs. The carpel surfaces were wrinkled, and sepals, petals, and stamens were small in size (Figures 6E and 6F). The aberrant floral organs formed at very early flower developmental stages, when narrowed sepals failed to enwrap the inner-whorl organs (Figure 6G). Mature *rdr6-3 as2-101* flowers also showed some needle-like sepals and petals (data not shown). The pleiotropic *rdr6-3 as2-101* phenotypes indicate that the *RDR6* gene is required for both vegetative and reproductive developmental processes.

miR165/166 Are Repressed by *RDR6*, *AS1*, and *AS2*

Both the differentiation of vascular tissue and the establishment of adaxial-abaxial polarity in Arabidopsis leaves are known to require the five class III HD-ZIP family genes: *PHB*, *PHAVOLUTA* (*PHV*), *REVOLUTA* (*REV*), *ATHB8*, and *ATHB15* (Baima et al., 1995, 2001; McConnell and Barton, 1998; McConnell et al., 2001; Emery et al., 2003; Ohashi-Ito and Fukuda, 2003; Dinneny and Yanofsky, 2004). Four of these genes share a region that is complementary to the sequence of miR165, whereas the same region of *ATHB15* matches the sequence of another miRNA, miR166 (Figure 7A). Because *PHB* is regulated by *AS1* and *AS2* (Lin et al., 2003; Xu et al., 2003) and *RDR6* and *AS1/AS2* synergistically regulate leaf adaxial-abaxial polarity and vascular development, we examined levels of miRNA165/166 and the five HD-ZIP transcripts in wild-type and *rdr6-3 as2-101* mutant leaves.

Because miR165 and miR166 differ by only one nucleotide (Figure 7A) and molecular hybridization may not be able to distinguish one from the other, the hybridization signals with the

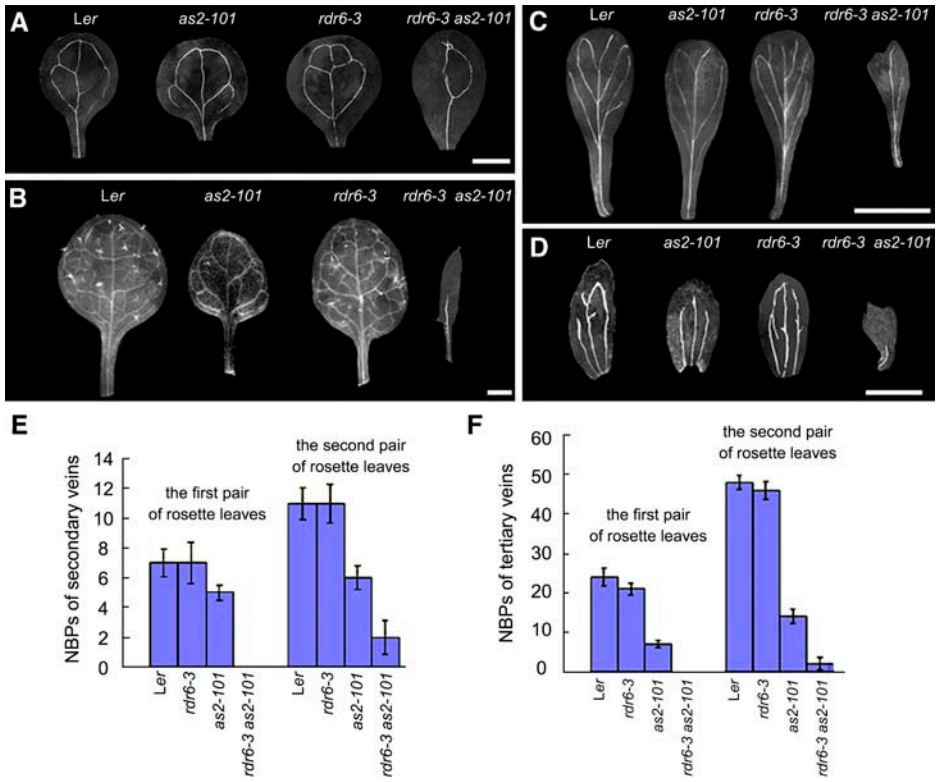

Figure 4. Abnormalities of Leaf Vascular Patterns of *rdr6-3 as2-101* Mutant Plants.

(A) Venations of cotyledons in wild-type, *as2-101*, *rdr6-3*, and *rdr6-3 as2-101* plants.
(B) Venations of the first rosette leaves in wild-type, *as2-101*, *rdr6-3*, and *rdr6-3 as2-101* plants.
(C) Venations of petals in wild-type, *as2-101*, *rdr6-3*, and *rdr6-3 as2-101* flowers.
(D) Venations of sepals in wild-type, *as2-101*, *rdr6-3*, and *rdr6-3 as2-101* flowers. Note that venations of all leaves, sepals, and petals became very simple in the *rdr6-3 as2-101* mutant plants.
(E) and **(F)** Quantitative analyses of NBPs in wild-type and *rdr6-3 as2-101* leaves. Bars show standard deviation. Secondary leaf veins **(E)**; tertiary leaf veins **(F)**.
All mutants are in the L*er* genetic background. Bars = 1 mm in **(A)** and **(B)** and 5 mm in **(C)** and **(D)**.

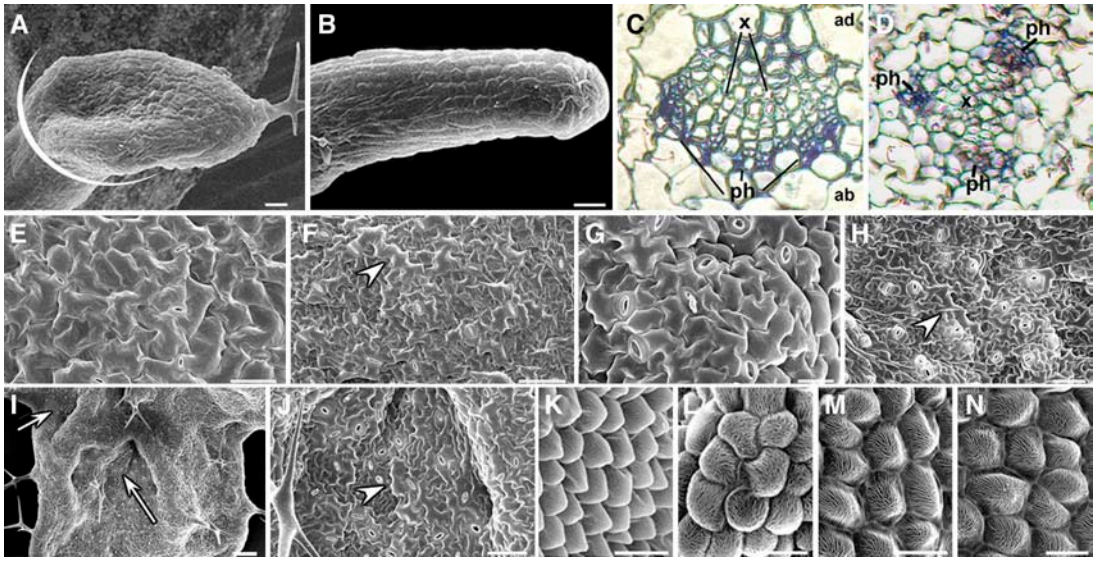

Figure 5. Aberrant Adaxial-Abaxial Polarity in Leaves and Petals of the *rdr6-3 as2-101* Mutant.

(A) A lotus leaf structure in *rdr6-3 as2-101* plants. White line indicates the approximate position where sections were prepared for images in **(C)** and **(D)**.
(B) A needle-like leaf in *rdr6-3 as2-101* plants. Note that lotus- and needle-like leaves reflect a severe loss of adaxial-abaxial leaf polarity.
(C) and **(D)** Transverse sections through petioles near the blade.
(C) Wild-type L*er*.
(D) *rdr6-3 as2-101* double mutant. x, xylem; ph, phloem.
(E) to **(J)** Epidermal patterns of leaves.
(E) Adaxial epidermis of wild-type L*er*.
(F) Abaxial epidermis of L*er*.
(G) *rdr6-3 as2-101* adaxial epidermis.
(H) *rdr6-3 as2-101* abaxial epidermis.
(I) Patches appeared on the adaxial side of an *rdr6-3 as2-101* leaf (arrows).
(J) A close-up of epidermal cells in a patch on the adaxial side of an *rdr6-3 as2-101* leaf.
(K) to **(N)** Epidermal patterns of petals.
(K) Adaxial epidermis of L*er*.
(L) Abaxial epidermis of L*er*.
(M) Adaxial epidermis of *rdr6-3 as2-101*.
(N) Abaxial epidermis of *rdr6-3 as2-101*.
Arrowheads in **(F)**, **(H)**, and **(J)** point a long and irregularly shaped cell that reflects the abaxial characters of a leaf. All mutant plants are in the L*er* genetic background. Bars = 25 μm in **(A)** and **(B)**, 50 μm in **(E)**, **(F)**, **(H)**, and **(J)**, 100 μm in **(I)**, 20 μm in **(G)**, **(K)**, and **(M)**, and 10 μm in **(L)** and **(N)**.

miR165 probe probably reflect the levels of both transcripts. miR165/166 transcripts were detected at low levels in the wild-type L*er* leaves, and their levels were increased slightly in *as1-101*, *as2-101*, and *rdr6-3* single mutant leaves (Figure 7B). Strikingly, the miR165/166 level in *rdr6-3 as1-101* and *rdr6-3 as2-101* double mutants was dramatically elevated (Figure 7B), indicating that *RDR6*, *AS1*, and *AS2* likely downregulate miR165/166. To test whether the *RDR6*, *AS1*, and *AS2* regulation was specific for miR165/166, we examined levels of miR157 and miR159, which are also expressed in leaves (Reinhart et al., 2002). We found that the accumulation of these two miRNAs did not differ between the wild-type and mutant plants (Figure 7B), indicating that not all miRNAs are affected by *RDR6*, *AS1*, and *AS2*.

To determine whether increased miR165/166 levels can cause cleavage of transcripts of class III HD-ZIP genes in leaves, we performed RT-PCR using gene-specific primers spanning the predicted cleavage site. Compared with the real-time RT-PCR products from L*er* leaves, those from *rdr6-3 as2-101* (Figure 7C, left) and *rdr6-3 as1-101* (Figure 7C, right) had decrease levels of *PHB*, *REV*, *ATHB8*, and *ATHB15* transcripts, whereas the *ATHB15* transcript, which does not completely match the miR165 sequence, was affected to a lesser extent. The *PHV* transcripts were not detected under our experimental conditions. To investigate whether the altered expression levels of these genes were also accompanied by changes in expression patterns, we performed *PHB* and *REV* in situ hybridization analyses. In wild-type plants, *PHB* and *REV* transcripts accumulated in the adaxial domain of a leaf primordium (Figures 7D and 7F). However, although *PHB* (Figure 7E) and *REV* (Figure 7G) transcripts were detected in the earlier-stage leaf primordium (arrowheads), they were reduced markedly in leaf primordia at the stage when leaf polarity began to establish. These results suggest that the increased miR165/166 levels may result in transcript degradations of the HD-ZIP genes.

Localization of miR165/166

It was previously reported that miR165 was accumulated in the abaxial domain of leaves, so that only transcripts of class III HD-ZIP genes in the abaxial domain were eliminated, whereas those in the adaxial domain can normally function to promote the adaxial cell fates (Kidner and Martienssen, 2004). However, this model could not explain why the increased miR165/166 levels (supposedly in the abaxial domain) resulted in degradation of class III HD-ZIP transcripts that are located in the adaxial domain in *rdr6-3 as2-101* leaves. To more clearly examine the localization of miR165/166 in leaf primordium, we performed in situ hybridizations using 4-concatenate copies of miR165 as a probe and following a protocol by Drews et al. (1991). At the torpedo stage, miR165/166 signals were detected throughout the entire embryo, with strongest hybridization in the distal parts of cotyledons and roots (Figure 8A). To our surprise, miR165/166 in the leaf primordium and young leaf did not show an abaxially accumulated pattern but was instead detected throughout the entire organ (Figure 8C). To ensure that this miR165/166 distribution pattern was correct, we repeated the in situ hybridization experiment using a different experimental protocol (Long and Barton, 1998). Again, miR165/166 signals were detected throughout the leaf primordia (Figure 8E). To avoid a potential artificial effect of the probe consisting of the 4-concatenate miR165 copies, we also used a sequence containing the predicted pre-miR165a sequence (Reinhart et al., 2002) as a probe to perform in situ hybridization experiments. Although the hybridization signals were very weak, they did not show a polar miR165/166 distribution (Figure 8G). miR165 sense probes did not produce hybridization signals under corresponding conditions (Figures 8B, 8D, 8F, and 8H). Taken together, our results reveal a nonpolar miR165/166 distribution pattern in leaf primordia, unlike that reported previously (Kidner and Martienssen, 2004).

FILAMENTOUS FLOWER Expression in *rdr6-3 as2-101* Leaves

Our previous work has shown that *rdr6-3 as2-101* mutant plants display abaxialized leaves (Figure 5) and the adaxial-promoting factors do not function properly (Figure 7). However, it is not known how abaxial-promoting factors, such as YABBY, might be affected in the double mutant leaves. To test for possible changes in *YABBY* gene functions in the abaxial fate of leaves, we analyzed the expression of a *YABBY* family member, *FILAMENTOUS FLOWER* (*FIL*), in the *rdr6-3 as2-101* mutant by RT-PCR. In comparison with wild-type, *as2-101*, and *rdr6-3* leaves, *FIL* transcripts were dramatically increased in the *rdr6-3 as2-101* leaves (Figure 9A). *FIL* is usually expressed in the abaxial side of leaves (Figure 9B) but was extended throughout the entire primordium (Figure 9C, arrow) or to the adaxial side of young leaves (Figure 9C, arrowheads) in the *rdr6-3 as2-101* double mutant. These results indicate that similar to *BP* and miR165/166, *FIL* is repressed by the *AS1-AS2* and *RDR6* pathways in leaf development.

Overexpression of *MIR165a*

The Arabidopsis genome contains two genes for miR165: *MIR165a* and *MIR165b* (Reinhart et al., 2002). To test whether an elevated level of miR165 affects leaf polarity and vein formation in *rdr6-3 as2-101*, we introduced a *35S*:*MIR165a* fusion into wild-type L*er*, *as2-101*, and *rdr6-3* plants. The increased miR165 levels in the transgenic plants were verified by RNA filter hybridization (see Supplemental Figure 2 online). The L*er* background yielded 27 transgenic lines showing similar phenotypes of varying severity. Generally, the rosette leaves of these plants were smaller and round, with leaf margins slightly curled downward, resembling the margins of *as1*/*as2* leaves (Figure 10A). The *as2-101* background yielded 27 lines with similar phenotypes to each other (Figure 10B). The leaf shape

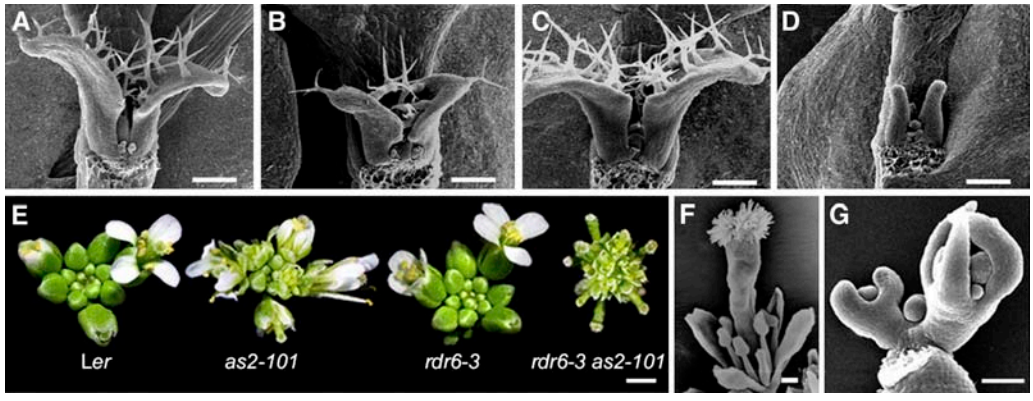

Figure 6. *rdr6-3 as2-101* Mutation Affects Other Developmental Processes.

(A) to **(D)** Six-day-old seedlings showed retarded rosette leaf growth in the *rdr6-3 as2-101* mutant. Wild-type L*er* **(A)**; *as2-101* **(B)**; *rdr6-3* **(C)**; *rdr6-3 as2-101* **(D)**.

(E) Inflorescence phenotypes of wild-type, *as2-101*, *rdr6-3*, and *rdr6-3 as2-101*.

(F) An *rdr6-3 as2-101* flower showing the short outer three whorls of organs.

(G) Abnormal flower phenotypes in the *rdr6-3 as2-101* mutant appeared during very early developmental stages, when sepals failed to enwrap the inner floral organs.

All mutant plants are in the L*er* genetic background. Bars = 80 μm in **(A)** to **(D)**, **(F)**, and **(G)** and 1 mm in **(E)**.

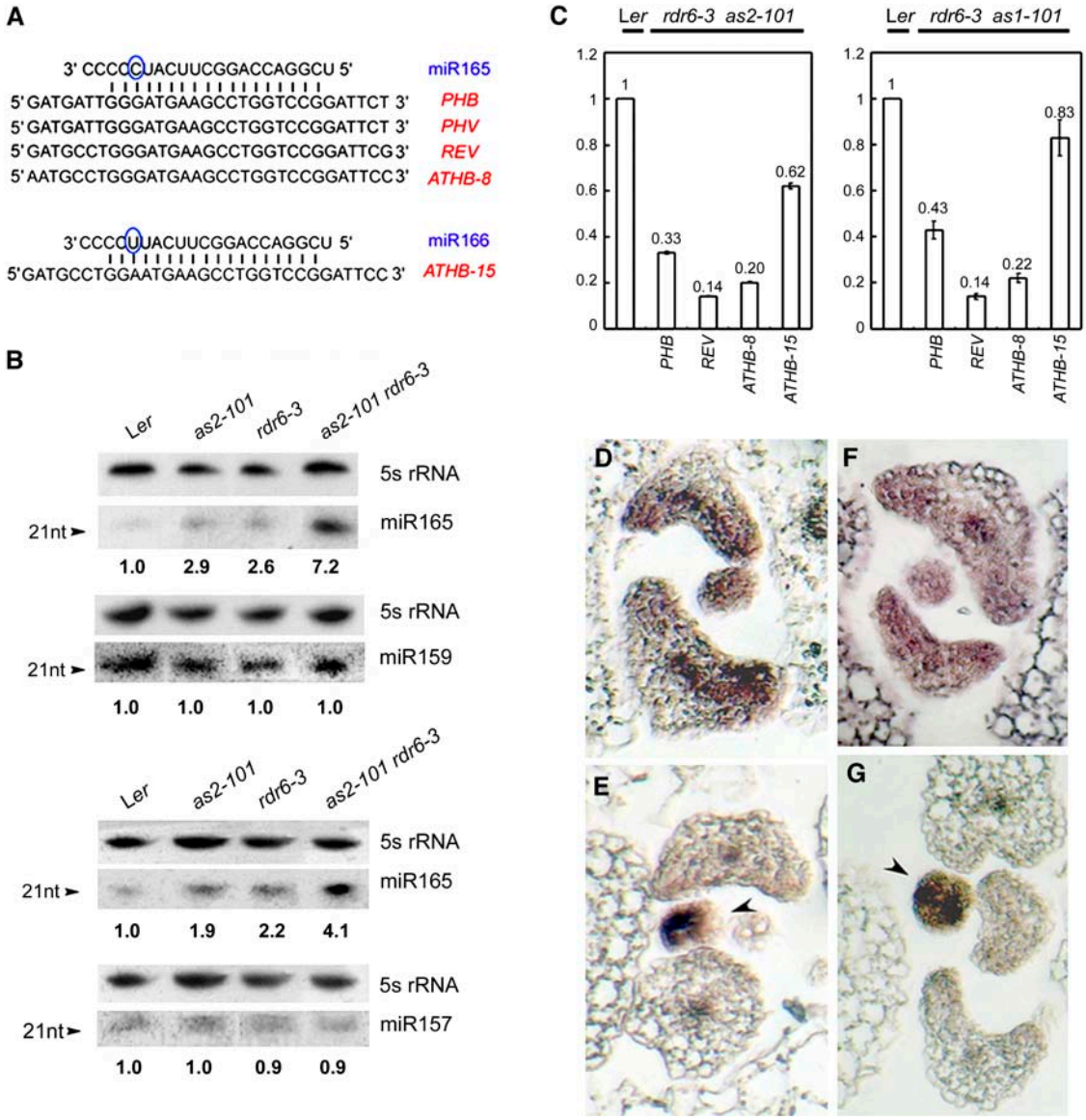

Figure 7. Analyses of Gene Expression.

(A) Sequences of miR165, miR166, and the region encoding the START domain of class III HD-ZIP proteins. Note that the circled C and U residues denote the nucleotide at which miR165 and miR166 differ.

(B) miRNA filter hybridizations. Lengths of RNA fragments in nucleotides (nt) and probes used in hybridizations are indicated on the left and right of each hybridization image, respectively. RNA gel blots were first probed by miRNAs, and the same filters were then analyzed by 5S RNA probe. Results were consistent from two separate experiments, using different preparations of RNA samples. Hybridization intensity was measured by phosphor image analysis, and the numbers indicate the relative abundance of miR165 levels, calculated using the band intensity of the first lane (L*er*) as 1.0.

(C) Steady state levels of mRNA of class III HD-ZIP genes in *rdr6-3 as1-101* (right) and *rdr6-3 as2-101* (left). RNA was quantified for the indicated mRNA by real-time RT-PCR using primers surrounding the cleavage site. Quantification was normalized to that of *ACTIN* and then to the value of the wild-type plants, whose value was arbitrarily fixed at 1. Bars show standard error.

(D) and **(E)** In situ hybridization using an antisense *PHB* probe on transverse sections of leaf primordia in wild-type L*er* **(D)** and *rdr6-3 as2-101* **(E)**.

(F) and **(G)** In situ hybridization using an antisense *REV* probe on transverse sections of leaf primordia in wild-type L*er* **(F)** and *rdr6-3 as2-101* **(G)**. Arrowheads indicate the earlier-stage leaf primordia. All mutants analyzed are in the L*er* genetic background.

was similar to that of *as2-101* plants, but the leaf surfaces became ruffled, similar to those of *rdr6-3 as2-101* double mutant leaves. In addition, these plants showed an increased frequency of lotus leaves compared with that in the *as2-101* plants (62% versus 1% of the first-pair rosette leaves, in plants grown on plates at 22°C). In comparison, the first pair of rosette leaves in 22 *35S:MIR165a/rdr6-3* transgenic lines resembled the expanded *as2-101* leaves, with down-curled leaf margins (Figure 10C; for comparison, see Figure 2B). Two other *35S:MIR165a/rdr6-3* lines displayed even stronger leaf phenotypes, showing lotus leaf structures (Figure 10D) or needle-like leaves with anthocyanin accumulation (Figure 10E). In addition to the abnormal leaf polarity, transgenic lines also showed reduced leaf venation (Figures 10F and 10G).

To investigate whether the altered leaf phenotypes in the transgenic plants are due to cleavage of class III HD-ZIP transcripts in a manner similar to that in the *rdr6-3 as2-101* mutant, we performed real-time RT-PCR using rosette leaves of the T2 generation of *35S:MIR165a/Ler* transgenic plants. In comparison with wild-type plants, the levels of *PHB*, *REV*, *ATHB8*, and *ATHB15* transcripts in the *35S:MIR165a/Ler* were reduced to varying degrees (Figure 10H), similar to those in *rdr6-3 as2-101* and *rdr6-3 as1-101* mutant plants (Figure 7C). The results from the *35S:MIR165a* transgenic plants strongly support the idea that an increased level of miR165 can affect leaf polarity and venation.

DISCUSSION

RdRP is an enzyme that uses single-stranded RNAs as templates to synthesize dsRNAs (Lipardi et al., 2001; Matzke et al., 2001; Nishikura, 2001; Sijen et al., 2001). Cleavage of dsRNAs by RNase III helicase (Dicer) generates small interfering RNAs (siRNAs), which are recruited by the RNA-induced silencing complex for PTGS/TGS of their cognate genes (Vaucheret et al., 2001; Aufsatz et al., 2002; Hutvagner and Zamore, 2002; Vaistij et al., 2002; Volpe et al., 2002). The biological functions of *RDR6* were previously thought to be associated with transgene silencing in transgenic plants (Dalmay et al., 2000; Mourrain et al., 2000; Vaistij et al., 2002) and virus resistance (Mourrain et al., 2000; Ahlquist, 2002). In this study, we demonstrate that the *RDR6* function is also required for the specification of pattern in the leaf. The fact that *RDR6* is involved in the mechanism for enhancing the *as1/2* mutant phenotype suggests that PTGS/TGS may be required for normal plant development.

as1 and *as2* mutant plants produce abaxialized leaves (Sun et al., 2002; Xu et al., 2002, 2003). We reported previously that expression of the *PHB* gene was enhanced in *35S:AS1/Ler* and

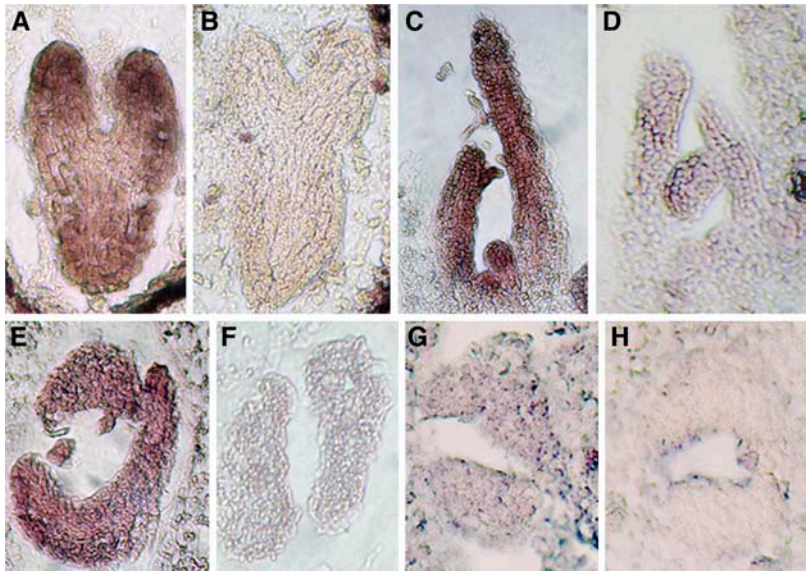

Figure 8. In Situ Localization of miR165/166 Expression in Wild-Type L*er* Plants.

Hybridizations were performed with the antisense miR165 probe (**[A]**, **[C]**, **[E]**, and **[G]**) or the sense miR165 probe (**[B]**, **[D]**, **[F]**, and **[H]**). In **(A)** to **(F)**, 4-concatenate miR165 was used as a probe. In **(G)** and **(H)**, pre-miR165 sequence was used as a probe.

(A) and **(B)** Torpedo-stage embryos. miR165/166 were detected throughout the entire embryo in **(A)**, but no signal was found in **(B)**.

(C) and **(D)** Longitudinal sections of plant vegetative apices. miR165/166 were expressed in the SAM, leaf primordial, and young leaves in **(C)** but were undetectable in **(D)**.

(E) and **(F)** Transverse sections of plant vegetative apices. miR165/166 hybridization signals were detected throughout the leaf primodia in **(E)**, but no signal was detected in **(F)**.

(G) Transverse sections of plant vegetative apices. miR165/166 signals were detected everywhere in the leaf primordium, though the signals were relatively weak.

(H) An antisense pre-165 could not detect miR165/166 signals.

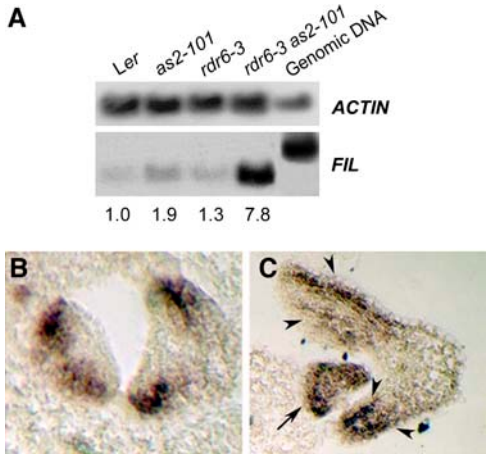

Figure 9. Expression of the *FIL* Gene.

(A) RT-PCR detection of *FIL* transcript levels in wild-type, *as2-101*, *rdr6-3*, and *rdr6-3 as2-101* leaves. Numbers indicate the relative abundance of gene transcripts and were calculated using band intensity of the first lane (L*er*) as 1.0.

(B) and **(C)** In situ hybridization using an antisense *FIL* probe to transverse sections of leaf primordia in wild-type L*er* **(B)** and *rdr6-3 as2-101* **(C)** that is in the L*er* genetic background. Note that the *FIL* expression was extended to the entire leaf primordium (arrow) and the adaxial side of young leaves (arrowheads).

35S:*AS2*/L*er* transgenic plants and that expression of the *FIL* gene was elevated in *as1-101* and *as2-101* mutant plants (Xu et al., 2003). These results, together with other data (Lin et al., 2003; Engstrom et al., 2004), suggest that *AS1* and *AS2* are genetically upstream of the *PHB* and *FIL* genes in the regulation of leaf polarity. However, it was not clear how *AS1* and *AS2* might influence these downstream genes for leaf polarity formation. In this work, we propose that (1) *AS1* and *AS2* upregulate the *PHB* and *REV* genes for specifying leaf adaxial identity via the repression of miR165/166, and (2) the *as1* and *as2* phenotypes might be caused at least partially by the altered transcript levels of HD-ZIP III genes.

This hypothesis is supported by two lines of evidence. First, miR165/166 levels were elevated in the *as1* and *as2* single mutants and were dramatically increased in the *rdr6 as1* and *rdr6 as2* double mutants. These miR165/166 accumulations may be accompanied by cleavage of transcripts from class III HD-ZIP family members. Second, overexpression of *MIR165a* in the *as2-101* and *rdr6-3* single mutants resulted in a more severe defect in adaxial-abaxial leaf polarity than that seen in the *as2-101* single mutant, indicating that the phenotype is a direct consequence of the change in miR165/166 content. Together, these data indicate that miRNA is an important link between *AS1-AS2* and class III HD-ZIP genes in the regulatory network of leaf development.

The proposed model that miR165 is accumulated in the abaxial domain of leaf primordium (Kidner and Martienssen, 2004) cannot explain some observations about class III HD-ZIP expression levels. For example, the *PHB* transcript level in the *phb-1d* mutant was elevated throughout the leaf, indicating that miR165/166 activities exist in the adaxial domain of leaf primordia (McConnell et al., 2001; Bao et al., 2004). Furthermore, the expression patterns of each class III HD-ZIP gene are distinguishable, with the *REV* transcripts in the more expanded range in the adaxial side of lateral organs than those of *PHB* and *PHV* (Emery et al., 2003) and the *ATHB-8* transcripts only in the vasculature (Baima et al., 1995). These results suggest that miR165/166 are not the sole factor affecting HD-ZIP distribution.

In this study, we report that miR165/166 are distributed throughout the leaf primordium. It is possible that miR165/166 expression may change over developmental stages of leaves. For example, according to the previous report, the miR165/166 distribution in P1-stage primordia seemed different from that in P2- and P3-stage primordia (Kidner and Martienssen, 2004). In fact, the miR165/166 distribution pattern in P1-stage primordia is similar to that of our in situ hybridization results, with signals in both adaxial and abaxial sides. In the older P2 and P3 primordia, signals became concentrated in the abaxial cells (Kidner and Martienssen, 2004). Additionally, we investigated whether the signal that is strongly accumulated in the cell walls of the abaxial domain of P2- and P3-stage primordia (Kidner and Martienssen, 2004) reflects a real cellular signal. Many previous in situ hybridization experiments using different probes indicated that signals at these stages of leaf primordia appear in the cytoplasm instead of in the cell walls (Bowman and Eshed, 2000; Byrne et al., 2000; Kerstetter et al., 2001; McConnell et al., 2001; Emery et al., 2003).

Our *35S*:*MIR165a* transgenic results showed that in addition to its function in the leaf polarity formation, miR165 may have other regulatory functions during leaf development, including vascular development and leaf shape control. These data also imply that miR165 may be required for the development of the entire leaf, not only the abaxial leaf domain. The Arabidopsis genome contains two miR165 and seven miR166 copies (Rhoades et al., 2002). It will be important in the future to determine the expression pattern for each of these miRNAs by miRNA promoter: reporter fusions, which may improve our understanding of their roles in leaf development.

We observed dramatically enhanced *FIL* gene expression in *rdr6-3 as2-101* mutant plants, with an expanded expression domain. Although it was previously proposed that the *PHB* pathway negatively regulates *YABBY* genes (Siegfried et al., 1999; Eshed et al., 2001; Bowman et al., 2002), our data suggest that the enhanced *FIL* expression may result from reduced HD-ZIP activity in the *rdr6-3 as2-101* mutant plants. Alternatively, the increased *FIL* transcripts in the *rdr6-3 as2-101* leaves may also result from defective PTGS/TGS, similar to those of *BP* and miR165/166.

Although it has been well documented that miRNAs play important roles in gene regulation in plants and animals, very little is known about how miRNA genes are regulated. Our data provide important information indicating that the *AS1-AS2* pathway and the *RDR6* pathway are both required for miR165/166 regulation. The *RDR6* and *AS1-AS2* pathways both negatively regulate *BP* and *MIR165/166*, but these regulations appeared to be processed separately. This idea was supported by the observation that *RDR6* expression in the *as1* and *as2* mutants and *AS1* and *AS2* expression in the *rdr6* mutant were not

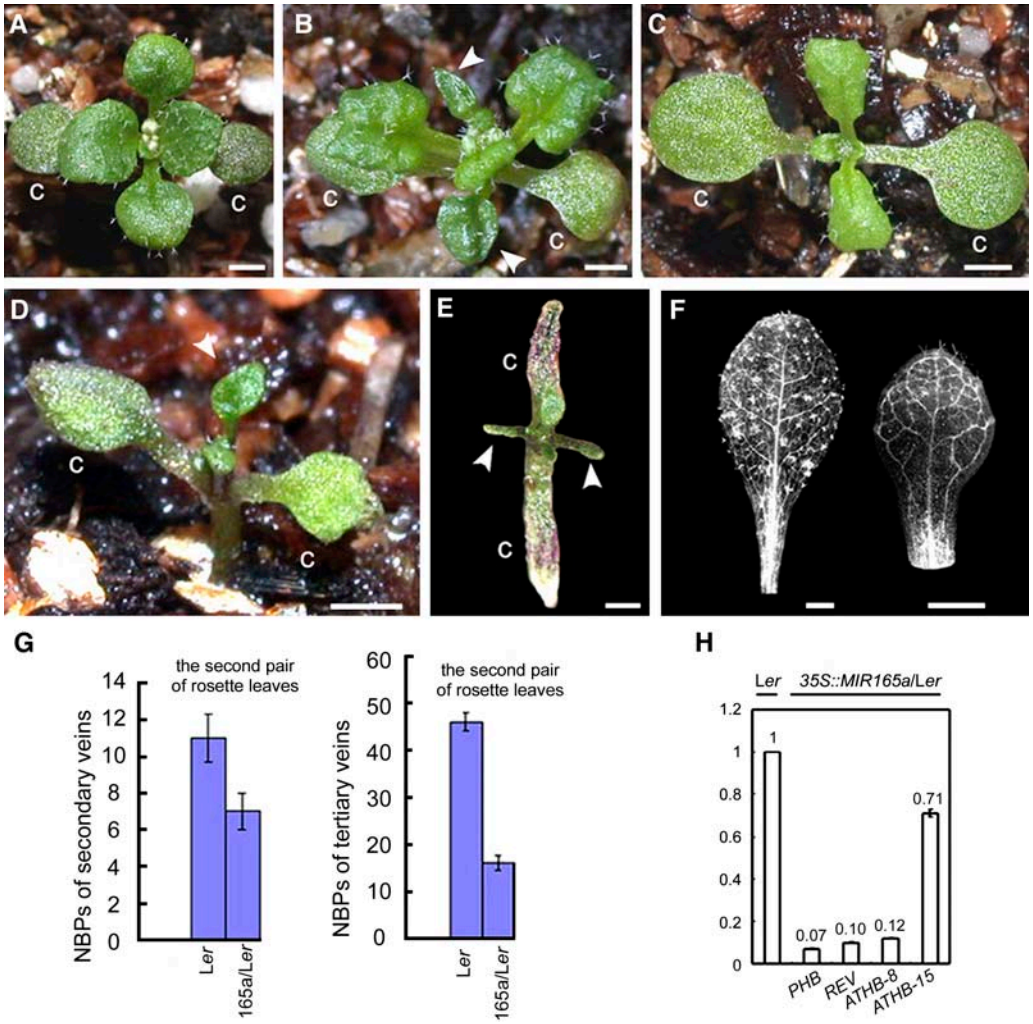

Figure 10. Phenotypes of *35S:MIR165a* Transgenic Plants.

(A) A *35S:MIR165a*/L*er* seedling, showing small and round leaves with margins slightly curled downward. C, cotyledon.
(B) A *35S:MIR165a/as2-101* seedling with ruffled leaf surfaces. Arrowheads indicate the lotus leaves.
(C) A *35S:MIR165a/rdr6-3* seedling. First-pair rosette leaves resemble those of the *as2-101* mutant plants.
(D) A *35S:MIR165a/rdr6-3* transgenic plant showing a lotus leaf structure (arrowhead).
(E) A *35S:MIR165a/rdr6-3* transgenic plant displaying severe phenotypes with abaxialized needle-like leaves (arrowheads).
(F) Comparison of venation between wild-type (left) and *35S:MIR165a*/L*er* (right) leaves, showing that venation of the *35S:MIR165a*/L*er* transgenic line was simplified. Bars = 1 mm in **(A)** to **(F)**.
(G) Quantitative analyses of NBPs in wild-type and *35S:MIR165a*/L*er* transgenic plants.
(H) Real-time RT-PCR to examine steady state levels of mRNA of class III HD-ZIP genes in wild-type and *35S:MIR165a*/L*er* plants. Bars show standard error.

obviously different from that in wild-type plants. However, the *rdr6 as2* double mutant showed much more severe phenotypes than either of the single mutants, indicating that the *AS1-AS2* and *RDR6* pathways may synergistically repress *BP* and *MIR165/166* in leaves. It is not clear how these two pathways act to regulate their downstream targets. One possibility is that in addition to the downregulation of *BP* and *MIR165/166* through the DNA binding function, AS1-AS2 may also be involved directly or indirectly in the generation of siRNAs used in the *RDR6* pathway to repress *BP* and *MIR165/166*. Alternatively, these two proteins might interact with or affect the regulation of AGO1, which is known to play a role in both the miRNA and siRNA pathways. AS1-AS2 functions may be so critical that plants with a loss of function in the *RDR6* gene do not show severe plant phenotypes. Although the *AS1-AS2* pathway is disrupted in the *as1* and *as2* mutants, the *RDR6* pathway can partially repress *BP* and *MIR165/166*. This regulation then attenuates the severity of plant phenotypes caused by *as1* and *as2* mutations. Plants with loss of function in both *AS1-AS2* and *RDR6* result in the abnormal *BP* and *MIR165/166* actions, leading to leaves with more severe

lobes, ectopic leaf primordia, and abnormal adaxial-abaxial polarity and venation.

METHODS

Plant Materials and Growth Conditions

Arabidopsis thaliana as1-101 and *as2-101* mutants in the L*er* background were generated as described previously (Sun et al., 2000, 2002; Xu et al., 2002). Seeds of *sde1* (Col-24) and a *BP*:*GUS* transgenic line (Col) were kindly provided by D. Baulcombe (John Innes Centre, Norwich, UK) and S. Hake (University of California, Berkeley, CA), respectively. For generation of *as2* enhancers, *as2-101* seeds (L*er*) were ethyl methanesulfonate mutagenized (0.1%), and ~40,000 M2 plants from 1395 M1 lines were screened. To test whether the enhanced *as2* phenotypes were due to a second site mutation, we pollinated the new mutant flowers with wild-type L*er* pollen. The F1 progeny showed wild-type phenotypes, and F2 plants segregated with a distribution of 295 wild type, 78 *as2-101*, and 27 enhanced mutants, close to a 12:3:1 ratio. This suggested that the phenotypic enhancement was due to a mutation in an unlinked gene and that the new mutation alone did not cause obvious phenotypic changes. We then analyzed F3 plants of F2 wild-type-like plants and identified 16 F3 families that did not segregate for *as2* mutants. We crossed one plant from each of these 16 families to *as2-101*. From these 16 crosses, one parent plant, whose 13 independent F2 families all yielded approximately one-sixteenth enhanced mutants, was considered to be the homozygous single *as2*-enhancing mutant. This plant was named *as2 enhancer1* (*ae1-1*), and only this plant or its progeny was used for further work. The *ae1-1 as2-101* mutant was backcrossed to wild-type L*er* five times before phenotypic analysis.

Allelism tests between the two enhancer mutants were performed by pollinating the *ae1-1* flowers with pollen from F1 plants of a cross between the second mutant and L*er*. A total of 91 F1 plants consisted of 47 wild-type-like plants, 24 *as2-101* mutants, and 20 enhanced plants, indicating that the two enhancer mutations were allelic. Therefore, the second *as2* enhancer mutant was designated *ae1-2 as2-101*.

Map-Based Cloning

Mapping of the *AE1* locus was performed by analysis of an F2 population from a cross between *ae1-1 as2-101* and the polymorphic Col ecotype. The *AE1* locus was mapped to the proximal arm of chromosome 3, near the simple sequence length polymorphic marker nga6. A set of simple sequence length polymorphic markers was used to detect polymorphisms between the Col and L*er* ecotypes, and the *AE1* locus was mapped to a 21-kb region (BAC T9C5), which contains seven predicted genes. Sequencing of these candidate genes from *ae1-1 as2-101* and *ae1-2 as2-101* revealed that a gene called *RDR6* (also called *SDE1* or *SGS2*) contained nucleotide substitutions that resulted in premature stop codons in both alleles.

For the complementation experiment, a 6.85-kb *Sca*I-*Xba*I genomic fragment containing the 4.0-kb *RDR6* gene plus 0.85 and 2.0 kb of upstream and downstream sequences, respectively, was isolated from TAC clone K1J14 and inserted into the pCAMBIA1301 transformation vector. We then transformed *ae1-1* mutant plants with this 6.85-kb *RDR6* fragment and examined the transgenic T1 plants for complementation of the *ae1* phenotype (the distorted young rosette leaves that appear in almost all *ae1* plants). Eleven independent transgenic lines were obtained, and seven of those showed complete rescue of *ae1* phenotypes. The transgenic plants were verified by PCR with one vector-specific primer (5′-TGATGGCATTTGTAGGAGC-3′) and one *RDR6*-specific primer (5′-TGCCCGAGAATCCAAATC-3′). Therefore, the *ae1-1 as2-101* and *ae1-2 as2-101* mutants were renamed *rdr6-3 as2-101* and *rdr6-4 as2-101*, respectively.

RT-PCR

RNA extraction was performed as described previously (Xu et al., 2003) with leaves from 20-d-old seedlings, and reverse transcription was performed with 1 μg total RNA using a kit (Fermentas, Vilnius, Lithuania). PCR was performed in the presence of the double-stranded DNA-specific dye SYBR green (Shenyou, Shanghai, China) following the manufacturer's instructions. Amplification was monitored in real time with the fluorometric thermal cycler Rotor-Gene 2000 (Corbett Research, Sydney, Australia). PCR was performed with the following gene-specific primers: 5′-TGTGGAGAATGGAACCAC-3′ and 5′-CTAGCAGAGTTCCTTTCC-3′ for *PHB* (exon4/exon7), 5′-ATCTGTGGTCACAACTCC-3′ and 5′-TAGCGACCTCTCACAAAC-3′ for *REV* (exon3/exon8), 5′-GCTACCACAGATACTAGC-3′ and 5′-TCGCAAGGTCTAATGAGG-3′ for *ATHB-8* (exon3/exon8), 5′-TCAAAGGCAACTGGAACC-3′ and 5′-GTGCAAGTACTTTGGGTG-3′ for *ATHB-15* (exon4/exon9), and 5′-TGGCATCA(T/C)ACTTTCTACAA-3′ and 5′-CCACCACT(G/A/T)AGCACAATGTT-3′ for *ACTIN*. For real-time PCR, quantifications of each cDNA sample were made in triplicate, and the consistent results from at least two separately prepared RNA samples were used. For each quantification, conditions were, as recommended, $1 \geq E \geq 0.80$ and $r^2 \geq 0.980$, where E is the PCR efficiency and r^2 corresponds to the correlation coefficient obtained with the standard curve. For each quantification, a melt curve was realized at the end of the amplification experiment by steps of 0.5°C from 55 to 99°C. Results were normalized to that of *ACTIN*. PCR experiments for *AS1*, *AS2*, and *RDR6* were performed with the following primers: 5′-CTGCGCCTCAACCGCCAATC-3′ and 5′-CCTTACATTACATTACAAGTTAC-3′ for *AS1*, 5′-TCCTCCGGCGAAAATGTC-3′ and 5′-CCGGCGAGTAAGTTGATGC-3′ for *AS2*, 5′-GGGACCTGTACTTTGTGGCTTGG-3′ and 5′-GGGCATGGACCAGATGTGACCC-3′ for *RDR6* (exon1/exon2), and 5′-CTTACTTCAATCCCCAGG-3′ and 5′-CTTTTGGACATGATAAACCC-3′ for *FIL* (exon2/exon7). The PCR products were then analyzed by gel electrophoresis, and the relative abundance of gene transcripts was calculated by the GIS-2016 image system (Tanon, Shanghai, China) using the first-lane product as 1.0.

Construction of *MIR165a* Transgenic Plants

For overexpression of *MIR165*, a 141-bp *MIR165a* precursor was PCR amplified using genomic DNA from L*er* plants with gene-specific primers 5′-GGGTTAAGCTATTTCAGTTG-3′ and 5′-AGAGGCAATAACATGTTGG-3′, confirmed by sequencing, and inserted into the pMON530 vector, downstream of the *35S* promoter. This construct was introduced into L*er*, *as2-101*, and *rdr6-3* plants by *Agrobacterium tumefaciens*–mediated transformation. The transgenic lines were verified by PCR using a *35S*-specific primer (5′-GCTCCTACAAATGCCATCA-3′) and a primer matching the *MIR165a* precursor sequence (5′-AGAGGCAATAACATGTTGG-3′). miR165 overexpression was confirmed by miRNA filter hybridization (see Supplemental Figure 2 online).

miRNA Filter Hybridization

Total RNA was extracted as described previously (Huang et al., 1995), and ~5 to 10 μg RNA per lane was separated on a denaturing 19% polyacryamide gel (18 × 16 cm) containing 8 M urea, with each of the sense strands used as a positive control. Antisense probes (5′-GGGGGATGAAGCCTGGTCCGA-3′ for miR165, 5′-GTGCTCTCTATCTTCTGTCAA-3′ for miR157, and 5′-TAGAGCTCCCTTCAATCCAAA-3′ for miR159) were ^{32}P-end labeled, and hybridization was performed according to the method described by Chen (2004).

Detection of GUS Activity and in Situ Hybridization

Histochemical detection of GUS activity was performed with 5-bromo-4-chloro-3-indolyl β-D-glucuronic acid (X-Gluc) as a substrate. Leaf tissue was placed in X-Gluc solution [750 μg/mL X-Gluc, 100 mM $NaPO_4$, pH 7, 3 mM $K_3F_3(CN)_6$, 10 mM EDTA, and 0.1% Nonidet P-40] under a vacuum for 10 min at room temperature, then incubated overnight at 37°C. In situ hybridizations were performed as previously described (Drews et al., 1991; Long and Barton, 1998) using 10-d-old seedlings. The probes were made from cDNA clones containing sequences from exons 4 to 7 for *PHB*, exons 2 to 7 for *FIL*, and exons 3 to 8 for *REV* or from a pGEM7Z(+) plasmid harboring a fragment of the 4-concatenate miR165 or a fragment of the predicted pre-miR165a (Reinhart et al., 2002).

Microscopy

Fresh tissue from wild-type and mutant plants was examined using a SZH10 dissecting microscope (Olympus, Tokyo, Japan) and photographed using a Nikon E995 digital camera (Nikon, Tokyo, Japan). Wild-type and mutant plant tissue was observed by scanning electron microscopy as previously described (Chen et al., 2000). Vascular patterns and vein numbers were analyzed with a Zeiss dissecting microscope (Jena, Germany) using the dark-field setting, according to our previously described methods (Sun et al., 2002).

ACKNOWLEDGMENTS

The authors thank D. Baulcombe and Plant Bioscience Ltd. for the *sde1-1* seeds, S. Hake for the *BP*:*GUS* transgenic seeds, Q. Lin and L. Pi for the *rdr6-4 as2-101* seeds, The Ohio State University Arabidopsis Stock Center for TAC clone K1J14, X. Gao, J. Mao, H. Dai, and Y. Dou for their assistance with the scanning electron microscopy, and H. Ma, S. Luan, X. Chen, G. Tang, and W. Shen for helpful discussions and critical reading of the manuscript. This research was supported by grants from the Chinese Administration of Science and Technology (863), the Chinese National Scientific Foundation (30421001, 30370751, and 90208009), and the Shanghai Scientific Committee to H.H.

Received April 12, 2005; revised May 25, 2005; accepted May 25, 2005; published July 8, 2005.

REFERENCES

Ahlquist, P. (2002). RNA-dependent RNA polymerase, viruses, and RNA silencing. Science **296,** 1270–1273.

Aufsatz, W., Mette, M.F., Winden, J.V.D., Matzke, A.J.M., and Matzke, M. (2002). RNA-directed DNA methylation in *Arabidopsis*. Proc. Natl. Acad. Sci. USA **99,** 16499–16506.

Baima, S., Nobili, F., Sessa, G., Lucchetti, S., Ruberti, I., and Morelli, G. (1995). The expression of the *Athb-8* homeobox gene is restricted to provascular cells in *Arabidopsis thaliana*. Development **121,** 4171–4182.

Baima, S., Possenti, M., Matteucci, A., Wisman, E., Altamura, M.M., Ruberti, I., and Morelli, G. (2001). The Arabidopsis ATHB-8 HD-Zip protein acts as a differentiation-promoting transcription factor of the vascular meristems. Plant Physiol. **126,** 643–655.

Bao, N., Lye, K.-W., and Barton, M.K. (2004). MicroRNA binding sites in *Arabidopsis* class III HD-ZIP mRNAs are required for methylation of the template chromosome. Dev. Cell **7,** 653–662.

Bartel, D.V. (2004). MicroRNAs: Genomics, biogenesis, mechanism, and function. Cell **116,** 281–297.

Bowman, J., and Eshed, Y. (2000). Formation and maintenance of the shoot special meristem. Trends Plant Sci. **5,** 110–115.

Bowman, J.L., Eshed, Y., and Baum, S.F. (2002). Establishment of polarity in angiosperm lateral organs. Trends Genet. **18,** 134–141.

Byrne, M.E., Barley, R., Curtis, M., Arroyo, J.M., Dunham, M., Hudson, A., and Martienssen, R.A. (2000). *Asymmetric leaves1* mediates leaf patterning and stem cell function in *Arabidopsis*. Nature **408,** 967–971.

Chen, C., Wang, S., and Huang, H. (2000). *LEUNIG* has multiple functions in gynoecium development in *Arabidopsis*. Genesis **26,** 42–54.

Chen, Q., Atkinson, A., Otsuga, D., Christensen, T., Reynolds, L., and Drews, G.N. (1999). The *Arabidopsis FILAMENTOUS FLOWER* gene is required for flower formation. Development **126,** 2715–2726.

Chen, X. (2004). A microRNA as a translational repressor of *APETALA2* in *Arabidopsis* flower development. Science **303,** 2022–2025.

Cogoni, C., and Macino, G. (1999). Gene silencing in *Neurospora crassa* requires a protein homologous to RNA-dependent RNA polymerase. Nature **399,** 166–169.

Dalmay, T., Hamilton, A., Rudd, S., Angell, S., and Baulcombe, D.C. (2000). An RNA-dependent RNA polymerase gene in *Arabidopsis* is required for posttranscriptional gene silencing mediated by a transgene but not by a virus. Cell **101,** 543–553.

Dinneny, J.R., and Yanofsky, M.F. (2004). Vascular patterning: Xylem or phloem? Curr. Biol. **14,** R112–R114.

Drews, G.N., Bowman, J.L., and Meyerowtiz, E.M. (1991). Negative regulation of the *Arabidopsis* homeotic gene *AGAMOUS* by the *APETALA2* product. Cell **65,** 991–1002.

Emery, J.F., Floyd, S.K., Alvarez, J., Eshed, Y., Hawker, N.P., Izhaki, A., Baum, S.F., and Bowman, J.L. (2003). Radial patterning of *Arabidopsis* shoots by class III HD-ZIP and KANIDI genes. Curr. Biol. **13,** 1768–1774.

Engstrom, E.M., Izhaki, A., and Bowman, J.L. (2004). Promoter bashing, microRNAs, and *Knox* genes. New insights, regulators, and targets-of-regulation in the establishment of lateral organ polarity in Arabidopsis. Plant Physiol. **135,** 685–694.

Eshed, Y., Baum, S.F., Perea, L.V., and Bowman, J.L. (2001). Establishment of polarity in lateral organs of plants. Curr. Biol. **11,** 1251–1260.

Hamada, S., Onouchi, H., Tanaka, H., Kudo, M., Liu, Y., Shibata, D., Machida, C., and Machida, Y. (2000). Mutations in the *WUSCHEL* gene of *Arabidopsis thaliana* result in the development of shoots without juvenile leaves. Plant J. **24,** 91–101.

Huang, H., Tudor, M., Weiss, C.A., Hu, Y., and Ma, H. (1995). The *Arabidopsis* MADS-box gene *AGL3* is widely expressed and encodes a sequence-specific DNA-binding protein. Plant Mol. Biol. **28,** 549–567.

Hudson, A. (2000). Development of symmetry in plants. Annu. Rev. Plant Physiol. Plant Mol. Biol. **51,** 349–370.

Hutvagner, G., and Zamore, P.D. (2002). A microRNA in a multiple-turnover RNAi enzyme complex. Science **297,** 2056–2060.

Iwakawa, H., Ueno, Y., Semiarti, E., Onouchi, H., Kojima, S., Tsukaya, H., Hasebe, M., Soma, T., Ikezaki, M., Machida, C., and Machida, Y. (2002). The *ASYMMETRIC LEAVES2* gene of *Arabidopsis thaliana*, required for formation of a symmetric flat lamina, encodes a member of a novel family of proteins characterized by cysteine repeats and a leucine zipper. Plant Cell Physiol. **43,** 467–478.

Kerstetter, R.A., Bollman, K., Taylor, R.A., Bomblies, K., and Poethlg, R.S. (2001). *KANADI* regulates organ polarity in *Arabidopsis*. Nature **411,** 706–709.

Kidner, C.A., and Martienssen, R.A. (2004). Spatially restricted microRNA directs leaf polarity through *ARGONAUTE1*. Nature **428,** 81–84.

Lin, W., Shuai, B., and Springer, P.S. (2003). The Arabidopsis *LATERAL ORGAN BOUNDARIES*-domain gene *ASYMMETRIC LEAVES2* functions in the repression of *KNOX* gene expression and in adaxial-abaxial patterning. Plant Cell **15,** 2241–2252.

Lipardi, C., Wei, Q., and Paterson, B.M. (2001). RNAi as random degradative PCR: siRNA primers convert mRNA into dsRNAs that are degraded to generate new siRNAs. Cell **107,** 297–307.

Long, J., and Barton, M.K. (1998). The development of apical embryonic pattern in *Arabidopsis*. Development **125,** 3027–3035.

Long, J.A., Moan, E.I., Medford, J.I., and Barton, M.K. (1996). A member of the *KNOTTED* class of homeodomain proteins encoded by the *STM* gene of *Arabidopsis*. Nature **379,** 66–69.

Mallory, A.C., Reinhart, B.J., Jones-Rhoades, M.W., Tang, G., Zamore, P.D., Barton, M.K., and Bartel, D.P. (2004). MicroRNA control of *PHABULOSA* in leaf development: Importance of pairing to the microRNA 5′ region. EMBO J. **23,** 3356–3364.

Matzke, M., Matzke, A.J.M., and Kooter, J.M. (2001). RNA: Guiding gene silencing. Science **293,** 1080–1083.

McConnell, J.R., and Barton, M.K. (1998). Leaf polarity and meristem formation in *Arabidopsis*. Development **125,** 2935–2942.

McConnell, J.R., Emery, J., Eshed, Y., Bao, N., Bowman, J., and Barton, M.K. (2001). Role of *PHABULOSA* and *PHAVOLUTA* in determining radial patterning in shoots. Nature **411,** 709–713.

Mourrain, P., et al. (2000). *Arabidopsis SGS2* and *SGS3* genes are required for posttranscriptional gene silencing and natural virus resistance. Cell **101,** 533–542.

Nishikura, K. (2001). A short primer on RNAi: RNA-directed RNA polymerase acts as a key catalyst. Cell **107,** 415–418.

Ohashi-Ito, K., and Fukuda, H. (2003). HD-Zip III homeobox genes that include a novel member, *ZeHB-13* (*Zinnia*)/*ATHB-15* (*Arabidopsis*), are involved in procambium and xylem cell differentiation. Plant Cell Physiol. **44,** 1350–1358.

Ori, N., Eshed, Y., Chuck, G., Bowman, J., and Hake, S. (2000). Mechanisms that control *knox* gene expression in the *Arabidopsis* shoot. Development **127,** 5523–5532.

Peragine, A., Yoshikawa, M., Wu, G., Heidi, L., and Poethig, R.S. (2004). *SGS3* and *SGS2*/*SDE1*/*RDR6* are required for juvenile development and the production of *trans*-acting siRNAs in *Arabidopsis*. Genes Dev. **18,** 2368–2379.

Reinhart, B.J., Weinstein, E.G., Rhoades, M.W., Bartel, B., and Bartel, D.P. (2002). MicroRNAs in plants. Genes Dev. **16,** 1616–1626.

Rhoades, M.W., Reinhart, B.J., Lim, L.P., Burge, C.B., Bartel, B., and Bartel, D.P. (2002). Prediction of plant microRNA targets. Cell **110,** 513–520.

Sawa, S., Watanabe, K., Goto, K., Kanaya, E., Morita, E.H., and Okada, K. (1999). *FILAMENTOUS FLOWER*, a meristem and organ identity gene of *Arabidopsis*, encodes a protein with a zinc finger and HNG-related domains. Genes Dev. **13,** 1079–1088.

Schiebel, W., Haas, B., Marinkovic, S., Klanner, A., and Sanger, H.L. (1993). RNA-directed RNA polymerase from tomato leaves. I. Purification and physical properties. J. Biol. Chem. **268,** 11851–11857.

Schiebel, W., Pelissier, T., Riedel, L., Thalmeir, S., Schiebel, R., Kempe, D., Lottspeich, F., Sanger, H.L., and Wassenegger, M. (1998). Isolation of an RNA-directed RNA polymerase-specific cDNA clone from tomato. Plant Cell **10,** 2087–2101.

Semiarti, E., Ueno, Y., Tsukaya, H., Iwakawa, H., Machida, C., and Machida, Y. (2001). The *ASYMMETRIC LEAVES2* gene of *Arabidopsis thaliana* regulates formation of a symmetric lamina, establishment of venation and repression of meristem-related *homeobox* genes in leaves. Development **128,** 1771–1783.

Siegfried, K.R., Eshed, Y., Baum, S.F., Otsuga, D., Drews, G.N., and Bowman, J. (1999). Members of the *YABBY* gene family specify abaxial cell fate in *Arabidopsis*. Development **126,** 4117–4128.

Sijen, T., Fleenor, J., Simmer, F., Thijssen, K.L., Parrish, S., Timmons, L., Plasterk, R.H.A., and Fire, A. (2001). On the role of RNA amplification in dsRNA-triggered gene silencing. Cell **107,** 465–476.

Smardon, A., Spoerke, J.M., Stacey, S.C., Klein, M.E., Mackin, N., and Maine, E.M. (2000). EGO-1 is related to RNA-directed RNA polymerase and functions in germ-line development and RNA interference in *C. elegans*. Curr. Biol. **10,** 169–178.

Sun, Y., Zhang, W., Li, F., Guo, Y., Liu, T., and Huang, H. (2000). Identification and genetic mapping of four novel genes that regulate leaf development in *Arabidopsis*. Cell Res. **10,** 325–335.

Sun, Y., Zhou, Q., Zhang, W., Fu, Y., and Huang, H. (2002). *ASYMMETRIC LEAVES1*, an *Arabidopsis* gene that is involved in the control of cell differentiation in leaves. Planta **214,** 694–702.

Sussex, I.M. (1954). Experiments on the cause of dorsal ventrality in leaves. Nature **174,** 351–352.

Sussex, I.M. (1955). Morphogenesis in *Solanum tuberosum* L: Experiment investigation of leaf dorsoventrality and orientation in the juvenile shoot. Phytomorphology **5,** 286–300.

Tang, G., Reinhart, B.J., Bartel, D.P., and Zamore, P.D. (2003). A biochemical framework for RNA silencing in plants. Genes Dev. **17,** 49–63.

Vaistij, F.E., Jones, L., and Baulcombe, D.C. (2002). Spreading of RNA targeting and DNA methylation in RNA silencing requires transcription of the target gene and a putative RNA-dependent RNA polymerase. Plant Cell **14,** 857–867.

Vaucheret, H., Beclin, C., and Fagard, M. (2001). Post-transcriptional gene silencing in plants. J. Cell Sci. **114,** 3083–3091.

Vaucheret, H., Vazquez, F., Crata, P., and Bartel, D.P. (2004). The action of *ARGONAUTE1* in the miRNA pathway and its regulation by the miRNA pathway are crucial for plant development. Genes Dev. **18,** 1187–1197.

Volbrecht, E., Reiser, L., and Hake, S. (2000). Shoot meristem size is dependent on inbred background and presence of the maize homeobox gene. Development **127,** 3161–3172.

Volpe, T.A., Kinder, C., Hall, I.M., Teng, G., Grewal, S.I.S., and Martienssen, R.A. (2002). Regulation of heterochromatic silencing and histone H3 lysine-9 methylation by RNAi. Science **297,** 1833–1837.

Waites, R., and Hudson, A. (1995). *phantastica*: A gene required for dorsoventrality of leaves in *Antirrhinum majus*. Development **121,** 2143–2154.

Xu, L., Xu, Y., Dong, A., Sun, Y., Pi, L., Xu, Y., and Huang, H. (2003). Novel *as1* and *as2* defects in leaf adaxial-abaxial polarity reveal the requirement for *ASYMMETRIC LEAVES1* and *2* and *ERECTA* functions in specifying leaf adaxial identity. Development **130,** 4097–4107.

Xu, Y., Sun, Y., Liang, W., and Huang, H. (2002). The *Arabidopsis AS2* gene encoding a predicted leucine-zipper protein is required for the leaf polarity formation. Acta Bot. Sin. **44,** 1194–1202.

Zgurski, J.M., Sharma, R., Bolokoski, D.A., and Schultz, E.A. (2005). Asymmetric auxin response precedes asymmetric growth and differentiation of *asymmertic leaf1* and *asymmetric leaf2* Arabidopsis leaves. Plant Cell **17,** 77–91.

Zhong, R., and Ye, Z. (2004). *amphivasal vascular bundle 1*, a gain-of-function mutation of the *IFL1*/*REV* gene, is associated with alterations in the polarity of leaves, stems and carpels. Plant Cell Physiol. **45,** 369–385.